Emergence of Excited-State Plasmon Modes in Linear Hydrogen Chains from Time-Dependent Quantum Mechanical Methods

A. Eugene DePrince, III, Matthew Pelton, Jeffrey R. Guest, and Stephen K. Gray

Phys. Rev. Lett. **107**, 196806 — Published 3 November 2011

DOI: 10.1103/PhysRevLett.107.196806

Excited-state plasmon modes in linear hydrogen chains from time-dependent quantum mechanical methods

A. Eugene DePrince, III, Matthew Pelton, Jeffrey R. Guest, and Stephen K. Gray
Center for Nanoscale Materials, Argonne National Laboratory, Argonne, IL 60439

Explicitly time-dependent configuration interaction theory is used to predict a new type of plasmonic behavior in linear hydrogen chains. After an intense ultrashort laser pulse brings the system into a broad superposition of excited states, the electronic dipole of the entire chain oscillates coherently, and the system is predicted to emit radiation at energies significantly lower than the first absorption band. A simple classical model accurately predicts the energy of this plasmon resonance for different hydrogen chain lengths and electron densities, demonstrating that collective, free-electron-like behavior can arise in chains of as few as 20 hydrogen atoms. The excitation mechanism for this plasmonic resonance is a highly nonlinear, multiphoton process, different from the linear excitation of ordinary surface plasmons.

Localized surface plasmons are collective excitations of conduction electrons in metal nanostructures and have a number of important applications including molecular sensing, medical therapy, and the manipulation of optical energy at the nanometer scale [1]. Plasmon resonances are generally considered as arising from the coherent oscillation of free electrons, reflecting semiclassical, bulk behavior of the material. The growing ability to produce monodisperse clusters consisting of small numbers of metal atoms, together with the ability to simulate ever-larger quantum-mechanical systems, has led to the questions of how large a system needs to be to support a plasmon and how this collective behavior arises from the interaction of individual atoms. A number of recent theoretical studies attempt to capture the emergence of plasmonic behavior in metallic systems, largely from the standpoint of linear-response time-dependent density functional theory (TDDFT) [2–6]. Real time TDDFT studies on one-dimensional sodium chains predict an optical transition from the ground state to the first excited state whose dependence on chain length agrees with classical predictions of plasmon frequencies [7–9]; however, these transitions cannot exhibit the fast dephasing and collective behavior characteristic of plasmons. Possible emergence of plasmon behavior can be found in the time-dependent configuration interaction (TDCI) study of small sodium clusters [10], with plasmon decay being associated with fast electronic thermalization.

Linear chains of hydrogen atoms provide the simplest and most computationally tractable system that has the theoretical possibility of exhibiting plasmonic behavior. A number of studies predict the existence of a metal-insulator transition as the spacing between the atoms in these chains is increased [11–14]. For interatomic spacings below this distance, a metallic hydrogen chain has the potential to support longitudinal plasmon resonances. In this Letter, we probe the emergence of plasmonic behavior in linear hydrogen chains by explicitly evolving the TDCI wave function. Upon excitation with an intense ultrashort laser pulse, we observe low-frequency oscillations in the instantaneous dipole moment that correspond to the collective motion of electron density across the whole chain. These plasmons are predicted to emit at frequencies that are considerably lower than the principal absorption peak, which corresponds to the transition between the ground and first excited states. This phenomenon differs from conventional plasmon oscillations in that the emission is associated with transitions among excited states in the hydrogen chain; we therefore refer to it as an *excited-state plasmon*.

Our calculations are based on the time-dependent Schrödinger equation

$$i\frac{d}{dt}\mathbf{c}(t) = \mathbf{H}(t)\cdot\mathbf{c}(t), \tag{1}$$

where $\mathbf{c}(t)$ is a column vector of complex components, and $\mathbf{H}(t)$ is the Hamiltonian matrix. Within the dipole approximation, the Hamiltonian is given by

$$\mathbf{H}(t) = \mathbf{H}_0 - \hat{\mu}\cdot\mathbf{E}(t), \tag{2}$$

where $\mathbf{H}_0$ is the electronic Hamiltonian, $\hat{\mu}$ is the dipole operator, and $\mathbf{E}(t)$ is the applied laser field. $\mathbf{E}(t)$ is taken to be a z-polarized (along the molecular axis) $\sin^2$-shaped pulse:

$$E_z(t) = E_0\,\sin^2(\pi t/\tau)\,\sin(\omega t), \quad 0 < t < \tau, \tag{3}$$

where τ is chosen to be 1 fs. Unless otherwise indicated, ω is chosen to be 4.624 eV, and the field strength, E_0, is 0.05 a.u (an intensity of 1.61×10^{13} W/cm^2). This short pulse is not tuned to any specific excitation energy; rather, its parameters are intended to excite electrons into a broad superposition of states.

The wave function is expanded in the configuration-interaction basis, truncated at the level of either single (TDCIS) or single and double (TDCISD) excitations. Eq. (1) is then numerically integrated with a stable and accurate 4^{th}-order symplectic integrator [15]. Each time step involves a number of Hamiltonian matrix - vector products. The space spanned by the wave function is

large: our largest TDCISD calculation spans the space of nearly 10 million eigenfunctions. The TDCI equations are implemented as a series of tensor contractions which can be accelerated with NVIDIA graphics processing units in a similar manner to that presented in Ref. [16].

Figure 1 shows the time evolution of induced charge density in a 50-atom hydrogen chain (H_{50}) after interacting with the incident optical pulse as predicted by the TDCIS method. The interatomic distance here is taken to be 1 Å, and the hydrogen atoms are described by the minimal STO-3G basis set, which places a 1s orbital on each atom. The pulse is sufficiently short and intense

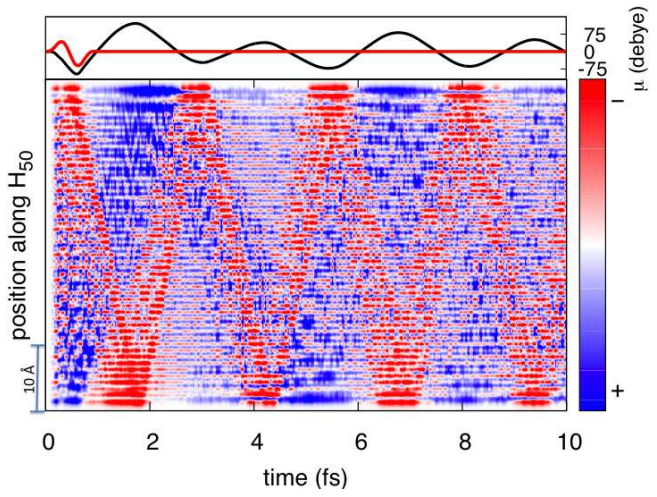

FIG. 1: (color online). Lower panel: Induced charge density in H_{50} as a function of time, as computed by the TDCIS method. The induced density is defined as the difference between the density before the pulse arrives and at time t, integrated over all x and y. Upper panel: dipole moment, μ, (black), and the shape of the incident optical pulse (red, arbitrary units).

to cause significant multiphoton absorption, leading to a broad superposition state of quasi-continuum, highly excited electronic states. The charge density oscillates repeatedly across the entire chain. This sort of collective charge oscillation is characteristic of a plasmon resonance in a metal nanostructure. The charge oscillations persist well after the end of the optical pulse and are associated with large oscillations in the dipole moment of the chain (also shown in Fig. 1).

An oscillating dipole moment results in radiation from the chain. Specifically, the square of the Fourier transform of the dipole acceleration (the second derivative of the dipole moment) can be interpreted as a scattering or emission spectrum. Figure 2 (a) shows the emission for H_{10} - H_{100}, again described by a minimal basis set with a 1 Å interatomic separation. For reference, the position of the principal absorption peak, corresponding to the transition between the ground and first excited states,

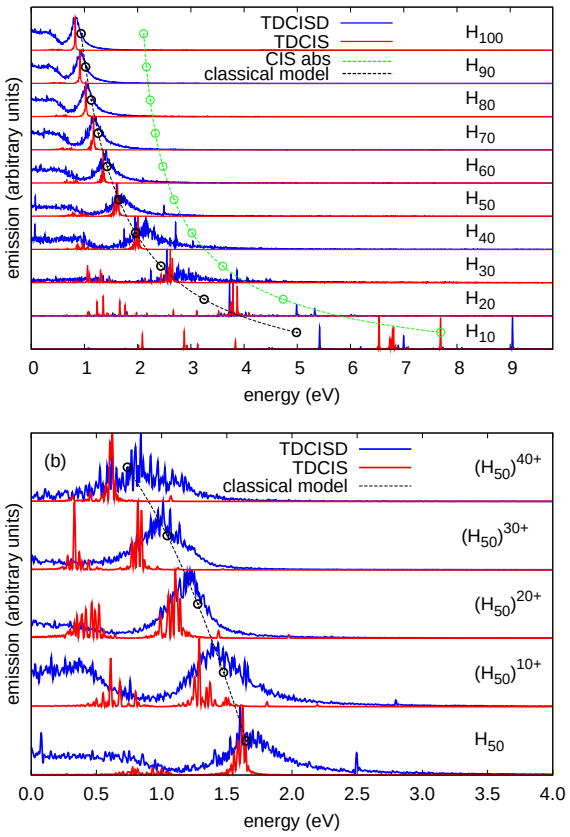

FIG. 2: (color online). Emission spectra computed by the TDCIS and TDCISD methods for hydrogen chains of varying length (a) and total electron density (b). Also shown are the positions of the first optical absorption peak (green) and the plasmon resonance as predicted by a classical model (black).

is also indicated in green. We also obtained very similar absorption behavior based on linear-response calculations with the time-dependent Hartree-Fock (TDHF) method.The emission spectrum for H_{10} is molecular in character: many features are present, but they are all isolated spectrally, and nothing resembling a plasmonic peak has emerged. For systems as small as H_{20}, however, the calculations show collective behavior, and, as expected, the plasmon peak red-shifts with increasing chain length. These features occur at very low energies, less than that of the first absorption, and can be interpreted as arising from simultaneous transitions between many excited states.

The TDCIS (red) and TDCISD (blue) methods predict similar positions for the plasmon resonance, suggesting that the wave function may be nearly converged with respect to the plasmon resonance energy with the inclusion of only single excitations. However, the inclusion of double excitations leads to a much broader resonance, a consequence of the larger density of excited states spanned by the CISD wave function. The spectra are inferred from 250 fs propagations, corresponding to 0.017 eV spec-

tral resolution; therefore the wide peak features are physically meaningful. Since loss via absorption or ionization is not included in our model, the peak widths are due to dephasing. The dephasing time for H_{100} from the TDCISD method is only ≈ 6 fs. Such fast dephasing times are comparable to the thermalization times inferred in TDCI studies of Na_8 clusters [10].

The plasmon resonance redshifts with increasing system size, as expected for an ordinary plasmon resonance in a metal wire. In fact, we can explain the peak position using a classical free-electron or Drude model [8]. The bulk plasma frequency is

$$\omega_p^2 = \frac{n_e e^2}{m_e \epsilon_0}, \tag{4}$$

where ϵ_0 is the permittivity of free space, n_e is the electron density, and e and m_e are the charge and mass the electron, respectively. We estimate the value of ω_p to be 20.7–21.8 eV for H_{10}-H_{100} with a 1 Å H-H spacing. By approximating the chain as a prolate spheroid and taking its dielectric constant to be $1 - \omega_p^2/\omega^2$, we arrive at the surface plasmon resonance frequency [17]:

$$\omega_{SP} = \omega_p \left(\frac{1-e^2}{e^2} \left(-1 + \frac{1}{2e} \ln \frac{1+e}{1-e} \right) \right)^{1/2}, \tag{5}$$

where the eccentricity, $e^2 = 1 - b^2/a^2$, depends on the semi-major and minor axis lengths, a and b, of the spheroid. The electron density in Eq. (4) is estimated by assuming all electrons are free and occupy a prolate spheroid of length $2a = (n-1) \times 1$ Å $+2b$ and maximum radius $b = 1.16$ Å; b is chosen so that the integral of the ground-state CIS density from a central atom in a direction x perpendicular to the molecular axis from $x = 0$ to b accounts for 95% of the integral from x=0 to ∞. The resonance positions predicted by Eq. 5 are denoted in black in Fig. 2. In general, we see good agreement between classical and *ab initio* resonance frequencies, with the best agreement for the largest systems. In addition to this size dependence, the classical model predicts that the plasma frequency, ω_p, and thus the plasmon resonance frequency, should depend on the density of conducting electrons. Figure 2 (b) confirms this prediction for various ions of H_{50}, where electrons are removed in order to decrease tthe electron density, n_e. No parameters in Eqs. (4) and (5) are adjusted in order to obtain this agreement.

As further evidence of the collective nature of the excited-state plasmon, we show that increasing the interatomic spacing in the chain leads to the disappearance of the resonance as the system goes through the metal-insulator transition. Fig. 3 illustrates the effect of changing interatomic spacing for H_{50} described by TDCISD methods in the larger 6-31G basis set which, in addition to the 1s orbital, places a 2s orbital on each hydrogen. First, we note that the effect of increasing the

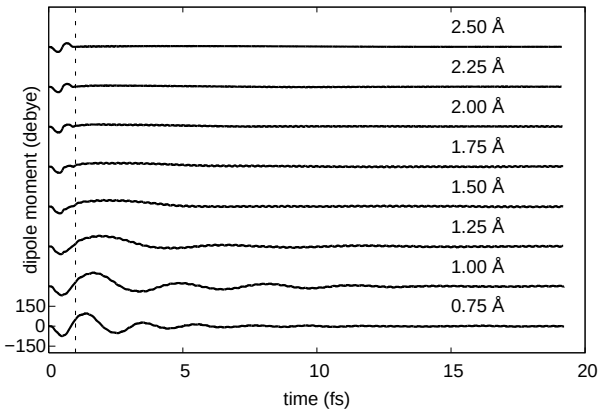

FIG. 3: Dipole moment as a function of time for various interatomic separations in H_{50}, as computed by the TDCISD method. The vertical dashed line at 1 fs denotes the end of the laser pulse.

basis set is insignificant; the frequency and rapid dephasing at 1 Å separations are very similar to those observed in the minimal basis set. This result indicates that the observed plasmon resonance is a real property of the system and not a consequence of an inadequate basis set. With increasing separation, the magnitude of the dipole oscillations decreases dramatically, vanishing altogether beyond 1.5 Å. In the isolated-atom limit, the only variations in the dipole moment occur during the pulse itself, with the electrons simply following the applied field.

The excited-state plasmon resonance is an intrinsic property of the system, showing little variation with respect to the chosen laser parameters. Figure 4 (a) illustrates the effect of field strength on the emission spectra from H_{50}, where the calculations use a STO-3G basis and the TDCIS method, and the the incident optical energy is 4.624 eV. In the weak-field limit ($E_0 = 0.001$ a. u.) the spectrum shows a single peak that corresponds to the energy difference between the ground and first excited states; the position of this peak is identical to that observed in a linear-response absorption spectrum. At high field strengths, the plasmon resonance appears. The energy of the plasmon peak is independent of field strength, provided that the fields are sufficiently intense to produce the nonlinear processes that result in this excited-state plasmon. The excited state plasmon peak position, ≈ 1.7 eV in this case, is also independent of the laser frequency, ω, as shown in Fig. 4 (b).

The dependence on field strength demonstrates that, although the plasmon resonance in these hydrogen-atom chains in many ways resembles ordinary surface plasmons in nanostructures, the excitation processes for the two phenomena are quite different. In an ordinary metal nanoparticle, linear interactions with an external field can excite plasmon oscillations directly from the ground state, due to a continuum of available states in the con-

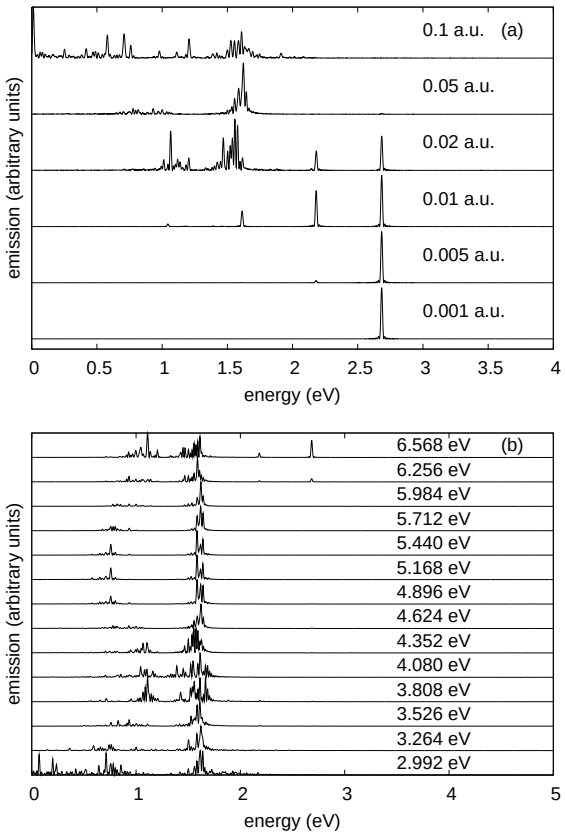

FIG. 4: Emission spectra for H_{50} after interacting with a laser field of varying strength (a) and energy content (b) as computed by the TDCIS method. The field strength, E_0, and frequency, ω, are given on the right.

duction band. In the case of hydrogen chains, by contrast, no such continuum of states is readily accessible from the ground state, the absorption spectrum being composed of discrete, isolated transitions. Instead, the excited-state plasmon is generated by forcing the system into a broad superposition of excited states with a dipole that oscillates at a relatively low frequency that corresponds to transitions among these states. It is particularly interesting that variations in the laser parameters result in very different final wave functions, and yet the excited-state plasmon resonance is found in exactly the same location in the respective emission spectra. For example, excitations with laser frequencies of 3.526 and 5.712 eV result in final wave functions, $|\Psi_1\rangle$ and $|\Psi_2\rangle$, that have an overlap, $|\langle\Psi_1|\Psi_2\rangle|$, of only 0.06. In a future study, it would be interesting to develop a better understanding of how the excited-state plasmon emerges from the superposition of atomic states created by the strong laser pulse, analogous to our understanding of standard, linear plasmon oscillations or our understanding of coherent-state dynamics for the quantum harmonic oscillator.

In conclusion, we predict the existence of a new type of plasmonic excitation in linear hydrogen chains within a fully *ab initio* and explicitly time-dependent framework. The position of the plasmon resonance, lower in energy than the first electronic transition from the ground state, is evidence that emission would involve transitions between excited states. The position of the resonance is determined only by the geometry of the chain and the total number of electrons; in particular, it is not sensitive to interactions between the atoms in the chain, as long as those interactions are strong enough that the chain is metallic (i.e., the interatomic spacing is below the critical spacing for the metal-insulator transition). The substantial width of the peak can be interpreted as arising from plasmon dephasing and reflects the large number of contributing electronic states. We show that the observed phenomenon is a collective one by demonstrating that the resonance vanishes entirely as the spacing between the hydrogen atoms is increased. The calculations demonstrate that collective, semiclassical electron oscillations can emerge in chains of as few as 20 hydrogen atoms, providing new insight into the transition from molecular to bulk-like behavior in mesoscopic systems. Although linear chains of hydrogen atoms are not readily accessible experimentally, it should be possible to adapt the present calculations to cover other atomic systems, and we expect that the predicted phenomenon will be quite general. In particular, future work will involve the study of chains of alkali or noble-metal atoms, which can be assembled on surfaces using scanning-tunneling-microscopy techniques and probed optically [18].

AED is supported by the Computational Postdoctoral Fellowship program at Argonne National Laboratory. This research used the "Dirac" GPU testbed system of the National Energy Research Scientific Computing Center, which is supported by the Office of Science of the U.S. Department of Energy under Contract No. DE-AC02-05CH11231. This research was supported by an allocation of advanced computing resources provided by the National Science Foundation. The computations were performed on Keeneland at the National institute for Computational Sciences (http://www.nics.tennessee.edu/). Use of the Center for Nanoscale Materials and the "Magellan" system of the Argonne Leadership Computing Facility were supported by the Office of Science of the U.S. Department of Energy under contract DE-AC02-06CH11357.

[1] M. Pelton, J. Aizpurua, and B. Garnett, Laser Photon. Rev. **2**, 136 (2008).
[2] K. Baishya, J. C. Idrobo, S. Ogut, M. Yang, and K. Jackson, Phys. Rev. B **78**, 075439 (2008)
[3] D. J. Masiello and G. C. Schatz, Phys. Rev. A **78** 042505 (2008).
[4] C. M. Aikens, S. Li, and G. C. Schatz, J. Phys. Chem. C

112, 11272 (2008).
[5] Z. Guo, B. F. Habenicht, W.-Z. Liang, and O. V. Prezhdo, Phys. Rev. B **81**, 125415 (2010).
[6] S. M. Morton, D. W. Silverstein, L. Jensen, Chem. Rev. **111**, 3962 (2011).
[7] J. Yan, Z. Yuan, and S. Gao, Phys. Rev. Lett. **98**, 216602 (2007).
[8] J. Yan and S. Gao, Phys. Rev. B **78** 235413 (2008).
[9] T. Yasuike, K. Nobusada, and M. Hayashi, Phys. Rev. A **83**, 013201 (2011).
[10] T. Klamroth and M. Nest, Phys. Chem. Chem. Phys. **11**, 349 (2009).
[11] J. Hachmann, W. Cardoen, and G. K.-L. Chan, J. Chem. Phys. **125**, 144101 (2006).
[12] T. Tsuchimochi and G. Scuseria, J. Chem. Phys. **131**, 121102 (2009).
[13] A. V. Sinitskiy, L. Greenman, and D. A. Mazziotti, J. Chem. Phys. **133**, 014104 (2010).
[14] D. A. Mazziotti, Phys. Rev. Lett. **106**, 083001 (2011).
[15] J. M. Sanz-Serna and A. Portillo, J. Chem. Phys. **104**, 2349 (1996).
[16] A. E. DePrince III and J. R. Hammond, J. Chem. Theory Comput. **7**, 1287 (2011).
[17] C. F. Bohren and D. R. Huffman, Absorption and Scattering of Light by Small Particles (Wiley, New York, 1983).
[18] G. Nazin, X. Qiu, and W. Ho, Phys. Rev. Lett. **90**, 216110 (2003).